

# Simulation of Lid Cavity Flow in Rectangular, Half-Circular and Beer Bucket Shapes using Quasi-Molecular Modeling

S. Kulsri, M. Jaroensutasinee, and K. Jaroensutasinee

**Abstract**—We developed a new method based on quasi-molecular modeling to simulate the cavity flow in three cavity shapes: rectangular, half-circular and bucket beer in cgs units. Each quasi-molecule was a group of particles that interacted in a fashion entirely analogous to classical Newtonian molecular interactions. When a cavity flow was simulated, the instantaneous velocity vector fields were obtained by using an inverse distance weighted interpolation method. In all three cavity shapes, fluid motion was rotated counter-clockwise. The velocity vector fields of the three cavity shapes showed a primary vortex located near the upstream corners at time  $t \sim 0.500$  s,  $t \sim 0.450$  s and  $t \sim 0.350$  s, respectively. The configurational kinetic energy of the cavities increased as time increased until the kinetic energy reached a maximum at time  $t \sim 0.02$  s and, then, the kinetic energy decreased as time increased. The rectangular cavity system showed the lowest kinetic energy, while the half-circular cavity system showed the highest kinetic energy. The kinetic energy of rectangular, beer bucket and half-circular cavities fluctuated about stable average values  $35.62 \times 10^3$ ,  $38.04 \times 10^3$  and  $40.80 \times 10^3$  ergs/particle, respectively. This indicated that the half-circular shapes were the most suitable shape for a shrimp pond because the water in shrimp pond flows best when we compared with rectangular and beer bucket shape.

**Keywords**—Quasi-molecular modelling, particle modelling, lid driven cavity flow.

## I. INTRODUCTION

THE lid driven cavity flow is one of the most studied fluid problems in computational fluid dynamics field because of the simple geometry with well-defined boundary condition and easily to code [1]. Owing to their broad range of natural, industrial and biomedical applications, cavity flows have been studied for years by both experimental and numerical investigation [2]. Lid driven cavity flow studies are useful to improve many practical application prototypes such as shortdwell coaters and melt-spinning processes in forming

Manuscript received November 30, 2006. This work was supported in part by This work was supported by Walailak University Fund and Yala Technical College to S. Kulsri, CX-KURUE and Computational Science Graduate Program, Walailak University for funding and computing facilities.

S. Kulsri is with the school of Science, Walailak University, Thasala, Nakhon Si Thammarat, 80161 Thailand. (e-mail: sit4012020@yahoo.com).

M. Jaroensutasinee is with the school of Science, Walailak University, Thasala, Nakhon Si Thammarat, 80161 Thailand. (e-mail: jmullica@wu.ac.th)

K. Jaroensutasinee is with the school of Science, Walailak University, Thasala, Nakhon Si Thammarat, 80161 Thailand. (e-mail: krisanadej@gmail.com)

continuous metal ribbons [3-4]. In addition, this knowledge could be applied to fundamental closed-streamline flow, improving manufacturing systems efficiency, and the study complex flow physics of constituting an ideal vehicle [5-6].

In the past, understanding of the recirculating flow within the cavity has been treated as one of the fundamental challenges for fluid dynamics researchers. Therefore, a number of studies have been performed extensively and the solutions for flow behaviours are carried out. Unfortunately, most of the previous studies [7-8] have been restricted to the analysis of fluid motion in squares, and only a few reports deal with the influence of cavity shape on the birth and evolution of recirculating flow structures. Most numerical simulations of the driven cavity flow use Navier-Stokes equations. Navier-Stokes equations are fundamental equations that govern fluid flow and can solve the dynamics of water flow [9-12].

Quasi-molecular modeling or particle models are a new numerical approach developed by Greenspan [13]. In this model, the number of molecules is scaled down from their actual values ( $\sim 10^{24}$ ) to smaller sizes (i.e. a small set of quasi-molecular particles which is approximately  $10\text{-}10^2$  particles), while the intermolecular forces are correspondingly adjusted to approximately the correct hydrodynamic situation in order to agree with classical molecular-type formulae and conserve both mass and normalized energy. Unlike the continuum and statistical mechanics approaches, this approach concerns non-steady state phenomena and variations in dynamical responses due to the variation of system parameters.

In this study, we focused on a prototype fluid problem (i.e. cavity problem). For simplicity we restricted our study to two-dimensional flow, even though our method is applicable in three dimensions as well. This allowed us to compare our results with the numerous numerical and experimental results available in the literature. This study aimed at (1) simulating a 2-D lid driven cavity flow in three cavity shapes: rectangular, half-circular and beer bucket, (2) studying the influence of cavity shape on the birth and evolution of recirculating flow structures and (3) comparing the internal energy in the system of the three cavity shapes. This comparison between three cavity shapes will be useful for designing a suitable shrimp pond shape that requires less energy and gives a maximum flow rate.

## II. MATERIALS AND METHODS

### A. Quasi-Molecular Modeling

We used quasi-molecular modeling to simulate the lid driven cavity flow in three cavity shapes: rectangular, half-circular and bucket beer. The physical response of the fluid was caused by external forces (i.e. molecular interaction) [13]. In quasi-molecular modeling, the interaction forces were considered only between nearest-neighbour particles and assumed to be the same form as in molecular dynamic (MD) modeling. The interaction force was represented by Eq. (1).

$$F(R) = \frac{G}{R^p} + \frac{H}{R^q} \quad (1)$$

Where  $G, H =$  parameters in particle structure  
 $p, q =$  exponential parameter in particle structure  
 $R =$  equilibrium position in particle structure

$G, H, p, q$  were positive constants with  $q > p$  in order to obtain the repulsive effect that was necessarily stronger than the attractive one. Molecular interaction forces had two components: attraction and repulsion. The four parameters  $G, H, p$  and  $q$  were yet to be determined. If  $p, q$  and  $R_0$  were given, then by conditions of mass and energy conservation,  $G$  and  $H$  were derived.  $R_0$  was the equilibrium distance of the quasi-particle structure.

Just as in MD modeling, the dynamical equation of motion for each particle  $P_i$  of the system was given by (2):

$$\frac{d^2 \vec{R}}{dt^2} = \sum_{\substack{j=1 \\ j \neq i}}^N \left( \frac{G}{R^p} + \frac{H}{R^q} \right) \frac{\vec{R}_{ij}}{|\vec{R}_{ij}|}, \quad i \neq j \quad (2)$$

Where  $\vec{R}_{ij} =$  the vector form of  $P_j$  to  $P_i$   
 $N =$  the number of particle

For the simulation of the lid driven cavity flow by quasi-molecular modeling, we chose  $p = 3, q = 5, R_0 = 0.2$  cm. The distance of local interaction  $D = 3$  cm. The motion of particle  $P_i$  was determined by the dynamical (3).

$$\frac{d^2 \vec{R}}{dt^2} = \sum_{\substack{j=1 \\ j \neq i}}^{1162} \left( -\frac{124024.3374}{R^p} + \frac{3.1006 \times 10^6}{R^q} \right) \frac{\vec{R}_{ij}}{|\vec{R}_{ij}|} \quad (3)$$

Our model solved this equation simultaneously with a leapfrog numerical scheme.

### B. Numerical Solution

In general,  $F_i = m_i \ddot{r}_i$  where  $i = 1, 2, 3, \dots, N$  could not be solved analytically from given initial data and had to be solved numerically. The choice of a numerical method was simplified by the physics of quasi-molecular modeling in

small time steps. The reason was that the repulsive component  $H/R^q$  in Eq. (5.1) could be treated accurately only with small time steps for small  $R$ , since  $H/R^q$  was unbounded as  $R$  went to zero. Therefore, the advantages of using a high order numerical method, which allowed the choice of large time steps in obtaining a high degree of accuracy, were not applicable in quasi-molecular modeling. The leapfrog formulas relating position, velocity and acceleration for particle  $P_i$  were as in Eq. (4)–(6).

$$v_{i,1/2} = v_{i,0} + (\Delta t / 2) \vec{a}_{i,0}, \quad (\text{starter formula}) \quad (4)$$

$$v_{i,k+1/2} = v_{i,k-1/2} + (\Delta t) \vec{a}_{i,k}, \quad k = 1, 2, 3, \dots \quad (5)$$

$$\vec{r}_{i,k+1} = \vec{r}_{i,k-1/2} + (\Delta t) \vec{v}_{i,k+1/2}, \quad k = 1, 2, 3, \dots \quad (6)$$

Where  $\vec{v}_{i,k}, \vec{a}_{i,k}$  and  $\vec{r}_{i,k}$  were the velocity, acceleration and position vectors of particle  $i$  at time  $t_k = k\Delta t$ ,  $\Delta t$  was the time step,  $\vec{v}_{i,k+1/2}$  was the velocity of particle  $i$  at  $t_k = (k+1/2)\Delta t$ , and so on.

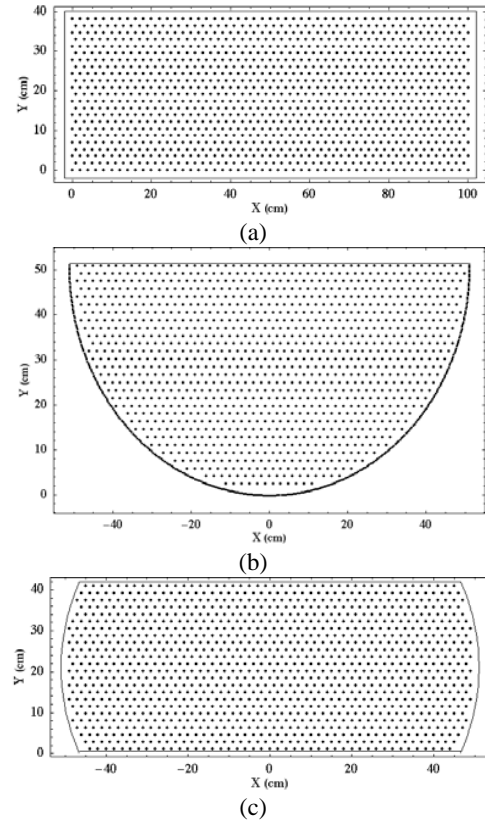


Fig. 1 Configuration of 1162 water particles in three cavities: rectangular, half-circular and beer bucket shapes

### C. Coordinate-System Setup

Three cavity shapes were setup: rectangular, half-circular and beer bucket while keeping a cavity area constant at 3800 cm<sup>2</sup>. A 2-D closed rectangular basin had a base of 100 cm and

height of 38 cm (Fig 1a). A 2-D half-circular basin was enclosed by a diameter of 100 cm. A 2-D half-circular basin was defined by the expression  $(x-p)^2 + (y-q)^2 = l^2$ , where a circle of radius ( $l$ ) = 50 cm and a center was located at (0, 51) (Fig 1b).

The sides of the basin in the three cavity shapes were called walls. The top wall alone was allowed to move in the  $X$  direction. The speed  $V$  of this top wall motion was called the wall speed (i.e.  $V = 10$  cm/s). In the basin, we constructed a regular triangular grid of 1162 points. The edge length of each triangular building block was 2 cm. At each grid point ( $x_i, y_i$ ), we set a particle  $P_i$ , that is, an aggregate of water molecules or a water particle (Fig 5.1). The water particles were distributed uniformly throughout the interior of the cavities. We assigned an initial random velocity over the interval  $[0, 0]$  to each particle in order to complete the initial data condition. The velocity vector fields were obtained by using an inverse distance weighted interpolation method, a technique for interpolation of scatter points [14].

### III. RESULTS AND DISCUSSIONS

Time sequences of instantaneous velocity vector fields from time  $t = 0.000$  to  $t = 1.500$  s for rectangular shape (Fig a-h), the half-circular shape (Fig 3a-h) and the beer bucket shape (Fig 4a-h) shown. The velocity vector fields were obtained by using an inverse distance weighted interpolation method, a technique for interpolation of scatter points [14]. In all three cavity shapes, fluid motion was rotated counter-clockwise (Fig 2a - h-4a-h). The velocity vector fields of three cavity shapes showed the development of a primary vortex located near the upstream corners (Fig 2a-h - 4a-h). Our results were in good agreement with previous simulation studies [15-17]. The vector field showed a primary vortex in three cavity shapes: rectangular, half-circular and beer bucket cavities located near the upstream corners at time  $t \sim 0.500$  s,  $t \sim 0.450$  s and  $t \sim 0.350$  s, respectively.

Our results showed that there was no secondary vortex in all three cavity shapes. In general, the secondary vortex is difficult to locate because the particles could be in motion and do not reveal themselves readily in a given velocity vector field [15-16]. With these constraints, it is very difficult to capture the secondary vortices in the simulation. From our previous study [17] on cavity flow in a square cavity shape, we captured a secondary vortex located in the lower right corner at  $t = 0.85000$  s. In the previous work, we set  $G = 12.402$  and  $H = 3.100$  in the dynamical equation as follow:

$$\frac{d^2 \bar{R}_i}{dt^2} = \sum_{j=1}^{1098} \left( -\frac{12.402}{R_{ij}} + \frac{3.100}{R_{ij}^3} \right) \frac{\bar{R}_j}{|R_{ij}|}$$

However, in this study, we set  $G = 124024.3774$  and  $H = 3.1006 \times 10^6$  in the dynamic equation as follow:

$$\frac{d^2 \bar{R}_i}{dt^2} = \sum_{j=1}^{1162} \left( -\frac{124024.3774}{R_{ij}} + \frac{3.1006 \times 10^6}{R_{ij}^3} \right) \frac{\bar{R}_j}{|R_{ij}|}$$

The reason that we used different value for  $G$  and  $H$  in this study was because we simulated a larger rectangular shape than in the previous study. Usually, a large rectangular cavity simulation requires a large number of particles and a super computer (or cluster or grids computing) to simulate. In order to be able to simulate this large rectangular cavity on a personal computer, we had to decrease the number of particles and increase the distance between particles. This allowed us to overcome the computational limit on a personal computer. There was no second vortex in the half-circular and beer bucket cavities because the curved walls of these cavities allowed particles to move easily.

Our study supported Migeon *et al.* [18]'s study, which experimentally studied the flow establishment in three cavity shapes: square, rectangular and half-circular cavities. They found that the square and rectangular cavities developed the primary and the secondary vortices and the half-circular cavity developed only the primary vortex, no secondary vortex. However, the half-circular cavity resulted in a much more homogeneous and uniform recirculation.

The kinetic energy in three cavity shapes increased as time increased until the kinetic energy reached its maximum at time  $t \sim 0.02$  s (Fig 5). Then, the kinetic energy in three cavity shapes decreased as time increased until the kinetic energy reached its steady state at time  $t \sim 0.20$  s (Fig 5). The kinetic energy started from zero at time  $t = 0.00$  s since we set the initial velocity of each particle is  $[0,0]$ . The half-circular cavity showed the highest kinetic energy (Fig 5). This highest kinetic energy in the half-circular cavity indicates that the particles in the half-circular cavity moved with the highest velocity when we compared with other cavities. On the other hand, the rectangular cavity system showed the lowest kinetic energy indicating the particles in this rectangular cavity moved slowest (Fig. 5).

The kinetic energy of the three cavities fluctuated about average values because the particles were in continual motion and colliding with one another. The positions and momentum of individual particles were continually changing. Therefore, most functions that depended on the positions and momentum were fluctuating. The kinetic energy of rectangular, beer bucket and half circular cavities fluctuated about average values of  $35.62 \times 10^3$ ,  $38.04 \times 10^3$  and  $40.80 \times 10^3$  ergs/particle, respectively (Fig. 5). This indicated that the half-circular shape was the most suitable shape for a shrimp pond because the water in shrimp pond flows best when compared with rectangular and beer bucket shapes. Time sequences of water droplet impact on smooth surface.

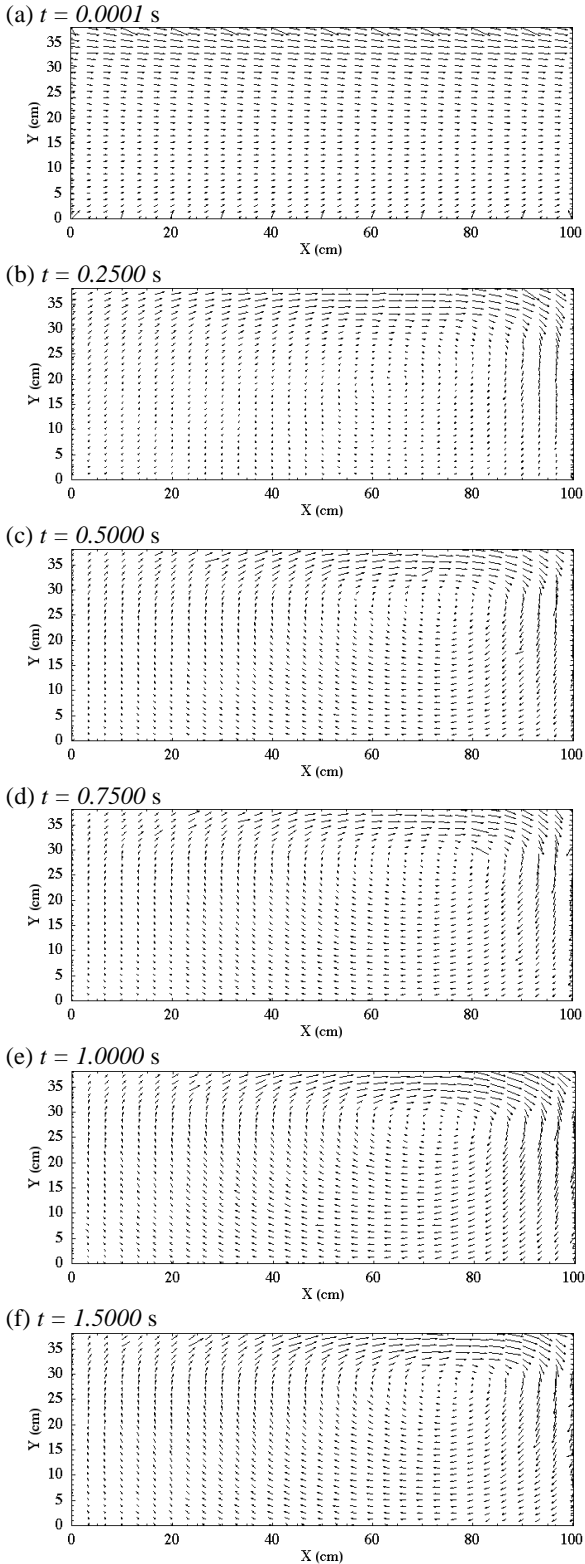


Fig. 2 Time sequences of instantaneous velocity vector field in rectangular cavity. (a)  $t = 0.0001$  s, (b)  $t = 0.2500$  s, (c)  $t = 0.5000$  s, (d)  $t = 0.7500$  s, (e)  $t = 1.0000$  s, and (f)  $t = 1.5000$  s

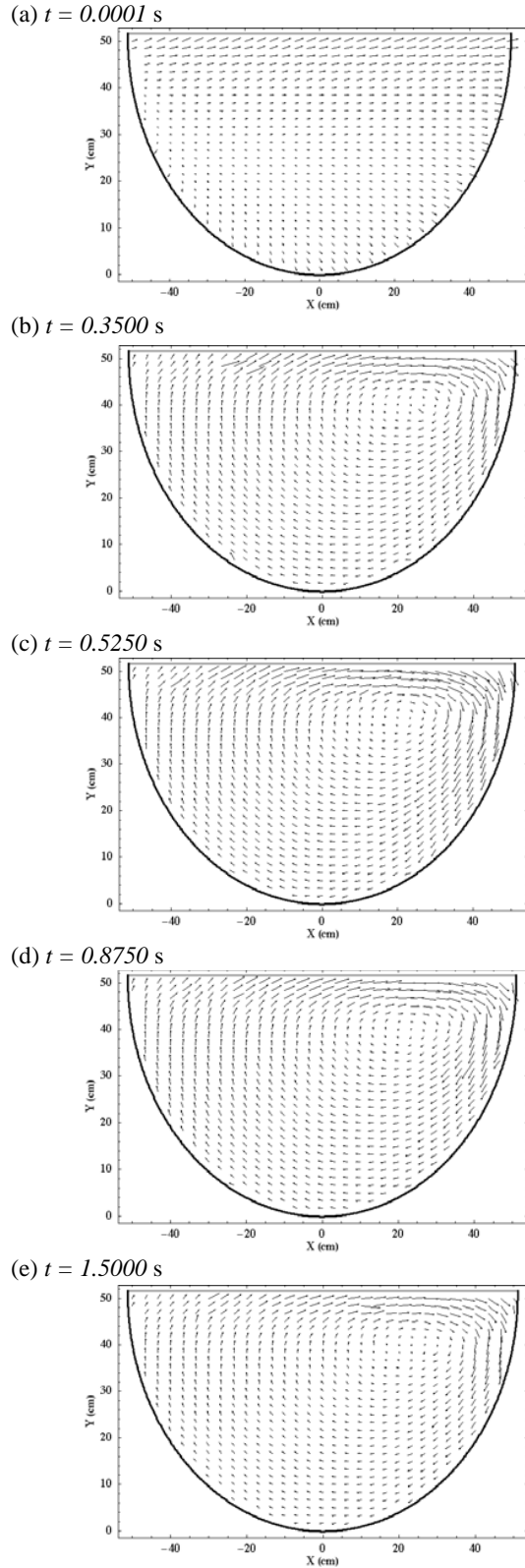


Fig. 3 Time sequences of instantaneous velocity vector field in half-circular cavity. (a)  $t = 0.0001$  s, (b)  $t = 0.3500$  s, (c)  $t = 0.5250$  s, (d)  $t = 0.8750$  s, and (e)  $t = 1.5000$  s

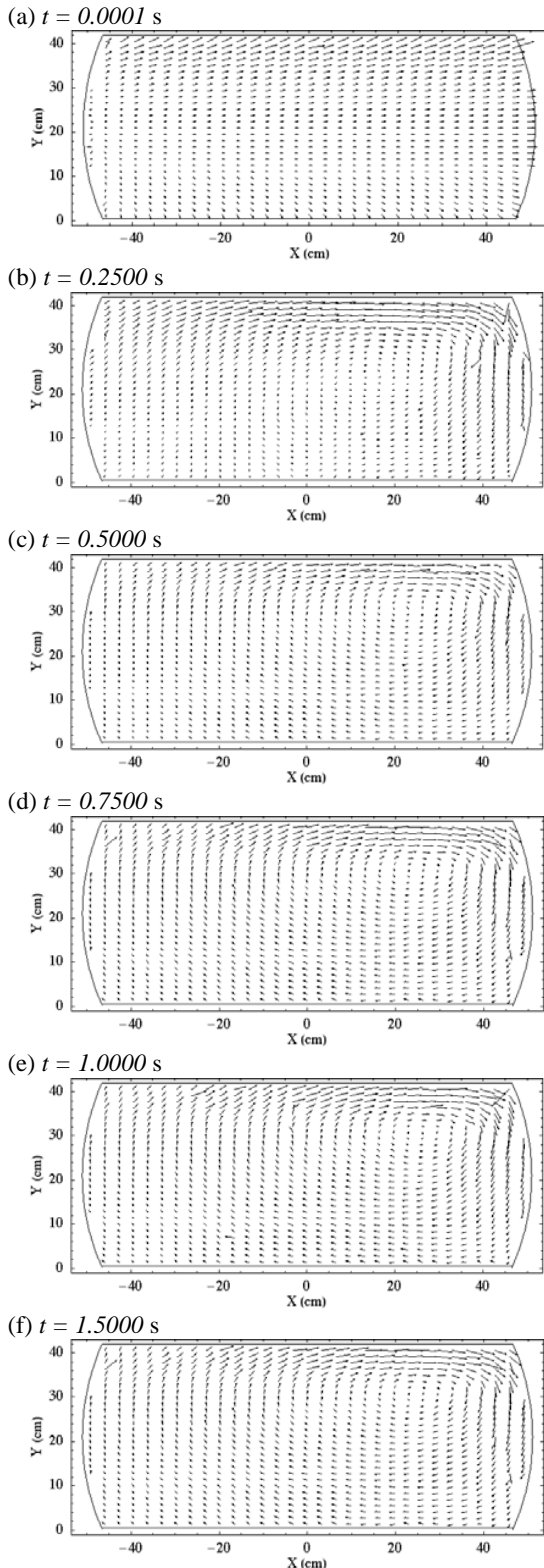


Fig. 2 Time sequences of instantaneous velocity vector field in beer bucket cavity. (a)  $t = 0.0001$  s, (b)  $t = 0.2500$  s, (c)  $t = 0.5000$  s, (d)  $t = 0.7500$  s, (e)  $t = 1.0000$  s, and (f)  $t = 1.5000$  s

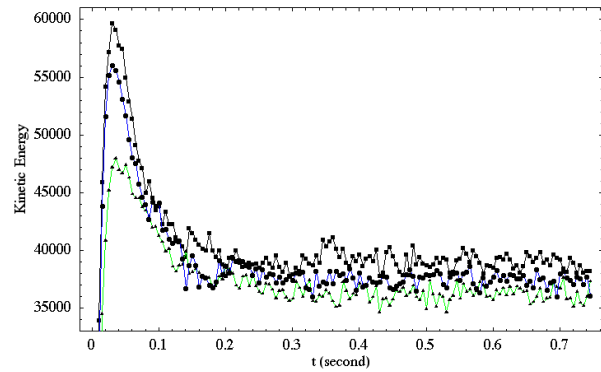


Fig. 5 The instantaneous kinetic energy (ergs/particle) from simulation of 1162 particles. ( $\blacktriangle$ ) rectangular shape, ( $\blacksquare$ ) half-circular shape, and ( $\bullet$ ) beer bucket shape

#### ACKNOWLEDGMENTS

This paper was a partial fulfilment of requirements for Ph.D. degree in Computational Science Graduate Program at Walailak University. We thank Asst. Prof. Dr. David Harding, and Dr. Pragasit Sitthitikul for useful comments on previous versions of the manuscript. This work was supported by Walailak University Fund and Yala Technical College to S. Kulsri, CX-KURUE and Computational Science Graduate Program, Walailak University for funding and computing facilities.

#### REFERENCES

- [1] E Erturk. "Nature of driven cavity flow at high Re and benchmark solution on fine grid mesh," *Int. J. Numer. Meth. Fluids*. Submitted for publication 2005.
- [2] A. J. Chorin. "Numerical study of slightly viscous flow," *J. Fluid Mech*, vol. 57, pp. 785-796, 1973.
- [3] C. K. Aidun, and N. G. Triantaflopoulos. In International symposium on mechanics of thin-film coating. Spring National Meeting of the AIChE. 1991.
- [4] C. K. Aidun, N. G. Triantaflopoulos and J. D. Benson, "Global stability of a lid driven cavity with through flow: flow visualization studies," *J. Phys. Fluids A*, vol.3, pp.2081-2091, 1991.
- [5] N. Ramanan, and G. M. Homsy., "Linear Stability of lid-driven cavity flow," *Phys. J. Phys. Fluids*, vol. 6, pp.2690, 1994.
- [6] C. J. Freitas, and R. L., "Street. Non-Linear Transport Phenomena in a Complex Recirculating Flow: A Numerical Investigation," *Int. J. Numer. Method Fluids*, vol. 8, pp 769-802, 1988.
- [7] U. Ghia, K. N. Ghia, and C. T. Shin, "High-Re Solutions for Incompressible Flow Using the Navier-Stokes Equations and a Multigrid Method," *J. Comp. Physics*, vol. 48, pp. 387-411, 1982.
- [8] V. M. Theodossiou and A. C. M., "Sousa. An efficient algorithm for solving the incompressible fluid flow equations," *Int. J. Numer. Meth. Fluids*, vol. 6, pp. 557-72, 1986.
- [9] A. J. Chorin, "Numerical study of slightly viscous flow," *J. Fluid Mech*, vol. 57, pp. 785-96, 1973.
- [10] J. Ehlers, K. Hepp and H. A. Weidmuller. Lecture note in physics #8. In: Proceeding of the 2<sup>nd</sup> International conference on numerical methods in fluid dynamics, New York, 1971.
- [11] A. E. Gill and K. Bryen, "Effect of geometry on the circulation of three-dimensional southern-hemisphere ocean model," *Deep-sea Research* vol. 18, pp. 685-721, 1971.
- [12] P. Jamet, P. Lascaux and P. A. Raviart, "Method de resolution numerique des equation de Navier-Stokes," *Numer. Math*, vol. 16, pp. 93-144, 1970.
- [13] D. Greenspan. *Quasi-molecular modelling*. JBW Printers and Binders Ptd. Ltd., Singapore, 1991.

- [14] Interpolation: inverse distance weighting, Available at: <http://www.ncgia.ucsb.edu/pubs/spherekit/inverse.html>, accessed March 2006.
- [15] D. Greenspan, "Particle Modelling of the cavity problem for liquids," *J. Com. Math. Appl.*, vol. 45, pp. 715-22, 2003.
- [16] D. Greenspan, "Molecular Mechanics-type approach to turbulence," *Math. Comput. Model.*, vol. 26, pp. 85-96, 1997.
- [17] S. Kulsri, M. Jaroensutasinee and K. Jaroensutasinee, "Simulation of lid cavity flow using quasi-molecular modeling," *Walailak J. Sci. & Tech.*, (to be published)
- [18] C. Migon, A. Texier, and G. Pineau, "Effect of lid driven cavity shape on the flow establishment phase," *J Fluid Struc.*, vol. 14, pp. 469-488, 2002.